The refractive index of $Al_xGa_{1-x}As$ below the band gap: Accurate determination and empirical modeling

S. Gehrsitz
Paul Scherrer Institut, Labor für Mikro-und Nanotechnologie, CH-5232 Villigen PSI, Switzerland

F. K. Reinhart and C. Gourgon
Institute de Micro-et Optoélectronique, EPFL, CH-1015 Lausanne, Switzerland

N. Herres
Fraunhofer Institut für angewandte Festkörperforphysik, Tullastrasse 72, D-79108 Freiburg i.Br., Germany

A. Vonlanthen and H. Sigg[a)]
Paul Scherrer Institut, Labor für Mikro- und Nanotechnologie, CH-5232 Villigen PSI, Switzerland

(Received 28 January 2000; accepted for publication 28 February 2000)

The refractive indices of $Al_xGa_{1-x}As$ epitaxial layers ($0.176 \leqslant x \leqslant 1$) are accurately determined below the band gap to wavelengths, $\lambda < 3$ μm. The layers are grown on GaAs substrates by molecular beam epitaxy metal organic and chemical vapor deposition with thicknesses ranging from 4 to 10 μm. They form improper waveguide structures with the GaAs substrate. The measurements are based on the excitation of the improper waveguide modes with grating couplers at 23 °C. The refractive indices of the layers are derived from the modal propagation constants in the range of 730 nm$<\lambda<$830 nm with an estimated uncertainty of $\Delta n = 5 \times 10^{-4}$. The temperature coefficient of the refractive index is investigated in the same spectral range. From the effective indices of the TE and TM modes, we derive the strain-induced birefringence and the elasto-optic coefficients. High-resolution x-ray diffraction is used to determine the strain of the layers. The layer compositions are obtained with inductively coupled plasma atomic emission spectroscopy. The measurement range of the refractive index is extended from the direct gap to $\lambda < 3$ μm by observing the Fabry-Pérot interference fringes of the transmission spectra of isolated layers. The measured values of the refractive index and the elasto-optic coefficient are compared to calculated data based on semiempirical models described in the literature. Published data of the index of refraction on GaAs, AlAs and GaP are analyzed to permit the development of a modified Sellmeier approximation. The experimental data on $Al_xGa_{1-x}As$ can be fitted over the entire composition range $0 \leqslant x \leqslant 1$ to provide an accurate analytical description as a function of composition, wavelength, and temperature. © *2000 American Institute of Physics.* [S0021-8979(00)04811-8]

I. INTRODUCTION

The semiconductor compound system $Al_xGa_{1-x}As/GaAs$ is an important material for the fabrication of optoelectronic devices. To design and fabricate waveguide devices, the refractive index has to be precisely known as a function of wavelength, composition, and temperature. Many attempts have been made by semiempirical models[1–8] to describe the index of refraction, n, as a function of the Al composition, x, and the wavelength, λ. The parameters of these models are simple functions of the composition. They are adapted to reproduce the available experimental data sets.[9–12]

Most of high accuracy refractive index measurements[10–15] were made on $Al_xGa_{1-x}As$ samples in the direct gap regime $0 < x < 0.37$. Aspnes *et al.*[11] report measurements on indirect gap samples, but with a lower accuracy of about 2%. The majority of these measurements also cover only a very limited wavelength range below the band gap. Measurements at the technologically important wavelengths of 1.3 and 1.5 μm were given by Deri[6] and van der Ziel.[13]

In this article, we describe an extensive study on the refractive index of several epitaxial $Al_xGa_{1-x}As$ layers grown by metal organic chemical vapor deposition (MOCVD) and by molecular beam epitaxy (MBE). The purpose of this study is to complement the available data and to increase the accuracy. The accuracy is dominated by the determination of the layer composition and the measurement technique. Thanks to the high precision of the measurement techniques, new data can be presented concerning the temperature dependence and the elasto-optic coefficients. The data are analyzed with a fitting procedure that permits us to describe the data analytically with high accuracy.

The article is organized as follows: in Sec. II, we introduce the measurement techniques based on waveguide and transmission or reflection techniques. The basic theory on the grating coupling technique with improper waveguides is reviewed, and the transmission method is briefly described. Potential error sources are estimated. The sample composition measurements are discussed. We compare the chemically determined Al concentrations with those obtained by

[a)]Author to whom correspondence should be addressed; electronic mail: hans.sigg@psi.ch

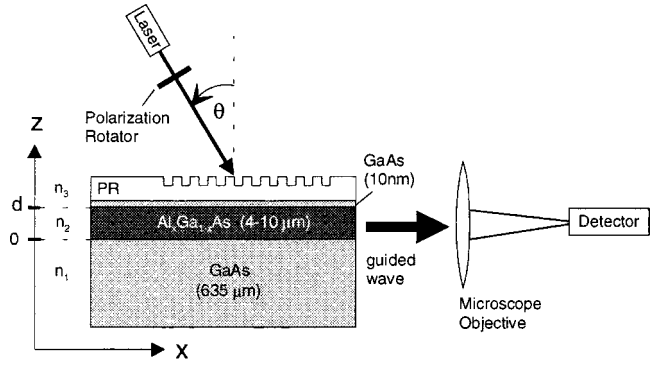

FIG. 1. Schematic sample structure and grating coupling experiment. The thickness of the layers is indicated by the number in brackets. The laser is a single frequency titanium sapphire laser operating in the 730–830 nm range. The detector, either a CCD camera or a photodiode, is positioned at the real image of the cleaved sample. PR: photoresist layer.

TABLE I. Parameters of the $Al_xGa_{1-x}As$ samples. The sample fabrication method is indicated by MOCVD and MBE. The chemical composition determined by ICP-AES is indicated with x_{ICP}. To permit comparison to published data, the Al composition determined from HRXRD under the assumption of Vegard's law, x_{XRD}, is listed along with the concentration obtained by optical means, $x_{OPTICAL}$. The layer thickness, d, is derived from the positions of the higher order modes observed in the angular scans of the grating coupling technique. The grating periodicity, Λ, is given for $T=23\,^{\circ}C$.

TYPE	x_{ICP}	x_{XRD}	x_{OPTIC}	$d/\mu m$	$\Lambda/\mu m$
MOCVD	0.176	0.193	0.170	5.1	0.255 08
MOCVD	0.334	0.368	0.325	10.4	0.246 34
MOCVD	0.410	0.438	0.405	4.2	0.246 36
MBE	0.427	0.455		3.8	0.246 11
MOCVD	0.615	0.646	0.619	9.0	0.250 41
MOCVD	0.753	0.779		5.0	0.250 11
MOCVD	0.865	0.869		4.9	0.248 40
MOCVD	0.998	1.000	1.000	7.8	0.250 09

optical and high-resolution x-ray diffraction (HRXRD) techniques. The HRXRD studies are also used to characterize the strain of the samples. In Sec. III, we analyze the published data on the binaries GaAs, GaP, and AlAs. The published AlAs data are complemented by our measurements. We develop a modified Sellmeier approach to fit the data. This empirical model is valid below the direct band gap and quite accurate. This analysis permits us to also develop a heuristic model to calculate the temperature dependence of the refractive index. The experimental results on $Al_xGa_{1-x}As$ are described and discussed in Sec. IV. First, we present the results of the refractive index measurements at room temperature using the model developed for the binaries. The high frequency dielectric constants are derived from the best data fits. By modifying the fitting parameters, we obtain an analytical expression for the refractive index dispersion of $Al_xGa_{1-x}As$ as a function of composition, wavelength, and temperature. The results on the piezobirefringence are also presented. The summary is given in Sec. V.

II. MEASUREMENT TECHNIQUES

A. The grating coupling technique with improper waveguides

In recent years, several groups employed the grating coupling technique for accurate refractive index measurements of semiconductor waveguide layers.[14–19] This technique is very accurate to determine the effective indices of the modes. The sample preparation is simple and nondestructive. In contrast to this previous work, we use improper waveguides that consist of a thick $Al_xGa_{1-x}As$ epitaxial layer on top of a GaAs substrate. In contrast to proper waveguides, there is no total internal reflection at the $Al_xGa_{1-x}As$/GaAs interface, since the refractive index of $Al_xGa_{1-x}As$ is lower than that of GaAs. However, the Fresnel reflectivity at this interface approaches unity for grazing incidence. This results in low reflection losses for the lowest order leaky modes. The simple structure thus supports leaky modes that gradually radiate their power into the GaAs substrate. Figure 1 schematically represents the improper waveguide structure. It consists of the GaAs substrate, the guiding $Al_xGa_{1-x}As$ layer, a thin protective GaAs cap, and a photoresist layer that contains the grating.

In the Appendix, A we give an approximate solution for the effective index and the attenuation coefficient for the leaky TE and TM modes. The model is based on a simplified three layer model with refractive indices n_1 and n_3 for the cladding layers (substrate and photoresist layer, respectively) and n_2 for the guiding layer material. For the effective index of the improper waveguide, we obtain in first order approximation the following relation (see Appendix):

$$n_{eff}=n_2[1-(1/2)\cdot(m\pi/n_2k_0d)^2], \tag{1}$$

where d is the thickness of the waveguide layer, and k_0 is the propagation constant of the light in vacuum. As is shown in the Appendix, the exact structure and the indices of the cladding layers are of minor importance for the determination of n_2. This fact is a consequence of the large thickness of the $Al_xGa_{1-x}As$ guiding layer.

The $Al_xGa_{1-x}As$ layers are 4–10 μm thick. They were grown by MOCVD or MBE on (100) GaAs substrates with a thin ($\sim$10 nm) GaAs cap layer. The samples are provided with a short period grating written into the positive photoresist (AZ 5214) over a lateral area of >10 mm^2. The gratings are defined with deep UV holography using a Lloyd interferometer. The UV source is a frequency doubled Ar^+-ion laser at $\lambda=257$ nm. Details on the grating fabrication process using reverse tone development are given in Refs. 20 and 21. The parameters of the samples are compiled in Table I.

The beam of a single-frequency Ti:sapphire laser (linewidth: 30 MHz) operating in the wavelength range between 730 and 830 nm is used to excite the guided modes via the grating. The beam diameter and the beam divergence are 3 mm and 0.03°, respectively. The power of the incident radiation is kept below 5 mW to avoid sample heating, since GaAs is opaque for wavelengths, $\lambda<870$ nm.

Figure 1 also schematically shows the experimental arrangement. The near field image of the modes is monitored with a charge coupled device (CCD) camera at the image of the cleaved edge of the $Al_xGa_{1-x}As$ layer formed with a

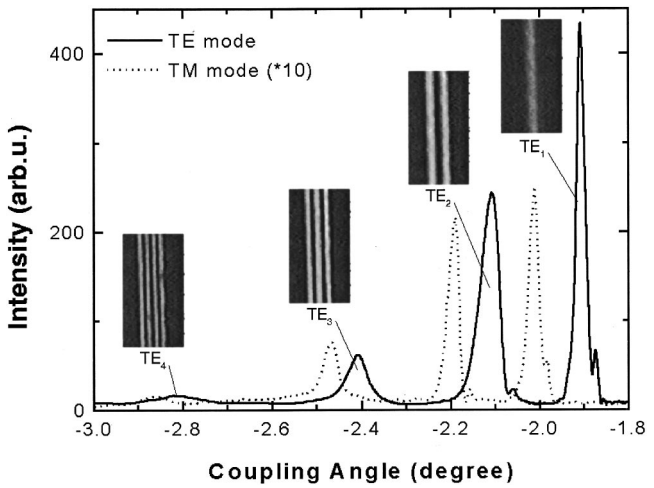

FIG. 2. Angular scan of sample with $x=0.753$ for the TE and TM modes at $\lambda=0.793$ μm and $T=23\,^{\circ}$C. The oscillations on the right hand side of the first and second order peak may be attributed to the leaky character of the modes and/or the limited aperture of the detection system. The insets show the corresponding near field images of the TE modes.

microscope objective. The intensity of the modes is determined with a photodiode. The coupling angle, ψ, is varied by rotating the sample mounted on a goniometer. Extremely sharp resonances can be observed at the grating coupling condition given by

$$n_{\mathrm{eff}}=\sin\psi_m+\lambda/\Lambda. \tag{2}$$

The resonance angle for the waveguide mode of order m is ψ_m. The grating period of the samples, Λ, is chosen to permit only the fundamental diffraction order.

Due to the narrow linewidth of the exciting laser light, we are able to resolve modes of the order $m\leqslant 4$. Figure 2 shows a typical scan for a 5-μm-thick $Al_{0.75}Ga_{0.25}As$ layer for the TE and TM modes. The insets represent the corresponding near field images observed with the CCD camera. As expected from theory, the intensity of the TM modes is reduced, because they experience higher radiation losses compared to the TE modes.

The very sharp resonances have a typical angular width at half maximum of approximately 0.025° for the first order mode. This fact permits us to determine the effective index with very high accuracy. From the position of the second and higher order modes ($m\geqslant 2$), it is possible to find the thickness of the guiding $Al_xGa_{1-x}As$ layer. If three or more modes can be observed, the film parameters of the simplified three layer model are over determined, and the positions of the higher order modes ($m>2$) can serve to cross check the layer thickness.

Several sources of error influence the accuracy of the index determination. The angular measurements are performed with a goniometer having an angular resolution of 0.01° and a reproducibility better than $\Delta\psi=0.02°$. The laser wavelength was determined with a Fizeau wavelength meter having an absolute accuracy of $\Delta\lambda=0.01$ nm. The grating period is measured with the same experimental setup, using the blue lines of an Ar^+-ion laser, with an accuracy of $\Delta\lambda=0.03$ nm. The combined error for the effective index sums up to be $\Delta n_{\mathrm{eff}}=4.7\times10^{-4}$. The sample temperature at 23 °C is controlled to $\Delta T=0.03\,^{\circ}$C.

The refractive index, n_2, of the guiding layer material is determined by correcting for the thickness dependence of n_{eff}. The correction for the fundamental mode is of the order of $\Delta n/n=1.5\times10^{-3}$ for a layer that is 4 μm thick. As seen from Eq. (1), the correction decreases with the square of $1/d$. The thickness obtained from the coupling angles of the higher order modes have a precision of approximately 2%. The correction due to the GaAs protection layer is estimated to be below 10^{-4}.

Hall measurements performed on the samples yield free carrier concentrations below $10^{17}\,\mathrm{cm}^{-3}$. Carrier induced changes of the refractive index are expected to be $<10^{-4}$.

B. Optical transmission measurements

To extend the wavelength range of the refractive index measurements, we perform transmission measurements on the thin films after separating them from the substrate by selective etching.[22,23] In these experiments, the thin films act as a Fabry-Pérot cavity and give rise to sharp fringes. The condition for maximum transmission is given by

$$2\cdot n\cdot t=j\cdot\lambda_j, \tag{3}$$

where j is an integer and t the effective geometrical thickness of the etched-off layer. To extract the index at the specific λ_j, it is necessary to know the thickness as well as the interference order j. The precision of the method is restricted, if the layer thickness can only be measured with limited accuracy. In our case, the refractive index dispersion between 0.73 μm and 0.83 μm is precisely known from the grating coupling measurements. This permits us to precisely determine t and j. The refractive index can thus be calculated for the complete spectral range of the transmission spectra. To reduce the uncertainty of λ_j, we fit the transmission data near the peaks and valleys with parabolas.

The spectra are acquired in normal incidence using a Perkin-Elmer Lambda 9 spectrophotometer. The slit width is chosen for a relative bandwidth of better than 0.2% in the wavelength range 0.4–1.5 μm. Above 1.5 μm, the relative wavelength resolution is reduced to about 0.5%.

C. Determination of the sample composition

The composition of the samples is specified by inductively coupled plasma atomic emission spectroscopy (ICP-AES) and HRXRD.[25,26] Optical measurements (photoluminescence and Raman scattering) are also used to provide comparisons to other published data. The ICP-AES technique provides the absolute Al content, x, by comparing the emission intensities of the atomic species forming the compound with standard solvents. The absolute measurement uncertainty is <0.005 for all values of x.

In contrast to the ICP-AES technique, HRXRD is an indirect method to characterize the composition, since it is based on the compositional dependence of the lattice constant. For the $Al_xGa_{1-x}As$ system, usually a linear relationship is assumed for the unstrained lattice constant as a func-

tion of the Al content (Vegard's law).[24] This assumption is not correct. The unstrained lattice parameters of our layers are calculated from the strained lattice constants perpendicular and parallel to the layer surface measured by HRXRD and the Poisson ratio measured by near infrared Brillouin scattering.[25,26] The relaxed lattice constant of GaAs at $T=22.5°C$ is $a_0=565.359$ pm. The best fit to the ternary $Al_xGa_{1-x}As$ lattice constant, $a_0(x)$, is given by[26]

$$a_0(x)=a_0+(0.921-0.112\cdot x)\cdot x \text{ pm} \quad \text{for } 0\leqslant x\leqslant 1. \tag{4}$$

Significant errors result in the concentration dependence of the lattice constant, if Vegard's law is assumed. It is worth noting that the composition values deduced from Vegard's law, x_{xrd}, provide an unambiguous relationship between data given in the literature and our data. The HRXRD measurements provide a fast, nondestructive method that can be performed routinely in almost every semiconductor laboratory with a high relative accuracy. The HRXRD data also yield a precise compositional analysis over the complete composition range (in contrast to photoluminescence or optical absorption measurements), and can provide additional information on the strain of the layer. A thorough discussion of this finding is given elsewhere.[26]

Some optical data are also given in Table I. Luminescence studies are quite easy to perform in the direct band gap regime of the materials. The calibration is also indirect, as one has to rely on primary standards given in the literature. In our case we have used those by Bosio *et al.*[27] For indirect gap materials, we have relied on Raman scattering data or on absorption spectra. No complete set of data is taken, because this method is also quite indirect.

III. ANALYSIS OF THE BINARIES AlAs, GaAs, AND GaP

A. Introductory remarks

The most precise index of refraction data of III–V compounds has been made with the minimum deviation method using bulk prisms. It is therefore of utmost interest to compare the available data with our results. Unfortunately, we can only compare our method in the case of AlAs, where transparent epitaxial layers of high quality can be grown on GaAs. Due to the chemical instability of AlAs only the waveguide technique can be employed. For GaAs, we rely exclusively on the data published by Marple.[9] Complete sets of data are available for three temperatures: 298, 185, and 103 K. Recently, Kisting *et al.*[16] published data on the temperature and wavelength dependence of the refractive index of GaAs. It is of great interest to compare these data sets. As GaP is electronically quite similar to AlAs, it is worthwhile to compare their dielectric properties. The data on GaP by Nelson and Turner[28] are particularly interesting, because of their high precision. Variations of the index of refraction on crystal preparation and doping levels were detected. However, no clear doping dependence could be established in spite of the fact that the variations from prism to prism are larger than the estimated measurement errors. These GaP data still seem to be the most precise ones among the III–V compounds. The question of the stoichiometry of III–V compounds influencing the index of refraction is still open.

If one looks at the wavelength and temperature dependence of a given material, the parameter range to be considered is quite large. Hence, it would be desirable to develop some kind of analytic relationship. Usually this is done by fitting the wavelength dependent data by some fitting formula. The Sellmeier fit has become the classical approach. However, the contribution of the direct transitions near the fundamental band gap is poorly described by the Sellmeier fit. Stern[1] carefully analyzed the contribution of the direct transitions to the dielectric function with the aid of the Kramers–Kronig (KK) relations. His aim was to obtain a realistic analytical function based on approximating the known absorption data near the band gap. In this fashion, he realized a reasonable prediction of the index of refraction through the band gap region. However, no explicit temperature dependence of the index of refraction dispersion was given. Later work[2,3,29] simplified the fundamental band gap contribution. These simplifications finally led to the unrealistic conclusion that the band gap contribution is logarithmic in nature.[29] It should be noted that in Stern's[1] approach a logarithmic term exists but in combination with an exponential integral. This combination renders the band gap contribution harmless, and it even remains small compared to contributions arising from other critical points. Unfortunately, this fact was overlooked in all subsequent articles. It is worthwhile to recapitulate the essential points from Stern's[1] calculation.

B. A fitting procedure to the index of refraction

Stern[1] pointed out that sufficiently far from a ''narrow'' absorption band at energy, E_i, the real part of the dielectric susceptibility, χ_i, can be represented by a term

$$\chi_i=\epsilon_0 G_i/(E_i^2-E^2), \tag{5}$$

where G_i is proportional to the oscillator strength, $E=hc/\lambda$ is the energy of the photon, ϵ_0 is the permittivity of the vacuum, h is Planck's constant, and c the light velocity in vacuum. Sufficiently far from an absorption band, the real part of the optical dielectric function, $\epsilon(E)$, is related to the index of refraction, n, and can be approximated by

$$n^2=\epsilon(E)/\epsilon_0=1+\sum G_i/(E_i^2-E^2) \quad \text{with } i=0,1,...N, \tag{6}$$

where the sum has to be extended over all $N+1$ absorption bands. This dielectric function is strictly correct, if the involved transitions are Lorentzian. Strong contributions to a KK integral arise only from steep gradients of the extinction coefficient. Indirect transitions show much weaker gradients than direct ones. For this reason, we do not consider indirect transitions. The dielectric function remains a good approximation even at energies above the lowest indirect transitions. Therefore, we restrict ourselves to energies below the direct band gap. As we do not precisely know the details of the important, contributing absorption bands nor their associated E_i, we propose for pragmatic reasons a modified Sellmeier fit

TABLE II. Parameters to determine n^2 of GaAs, AlAs, and GaP. All fits are made to published data described in the text by correcting for the contribution of the reststrahl band. The relative high frequency dielectric constants, n_∞^2, are given along with the standard deviation, σ, and the absolute value of the largest deviation, $\Delta n_{\max}$, between the experimental data and the fit. Two sets of fits for GaAs are shown to demonstrate that large variations of the fitting parameters do not strongly affect the quality of the fitting. All fits are made by setting E_0 to the direct band gap of the respective material. For GaAs, the experimentally determined temperature coefficients of A and E_1 are also given in the lower part of the table.

	GaAs FIT 1			GaAs FIT 2			AIAs	GaP
T/K	298	185	103	298	185	103	296.2	297.7
A	7.471	7.427 9033	7.390 927	6.090 524	6.06143	6.025 077	2.185 76	2.4782
$C_0/(\mu\text{m})^2$	0.015 381	0.015 381	0.015 381	0.019 788	0.019 788	0.019 788	0.0721	1.151 45
$E_0^2/(\mu\text{m})^2$	1.321 079	1.416 2842	1.475 453	1.321 079	1.416 284	1.475 453	5.8777	5.5
$C_1/(\mu\text{m})^2$	12.3615	12.3615	12.3615	21.5647	21.5647	21.5647	73.908	77.723 99
$E_1^2/(\mu\text{m})^2$	3.578 449	3.682 4591	3.740 014	4.500 042	4.610 738	4.669 352	12.4	12.1
$10^3\cdot C_2/(\mu\text{m})^2$		1.55			1.55		2.61	2.61
$10^3\cdot E_2^2/(\mu\text{m})^2$		0.724			0.724		1.331	1.331
n_∞^2	10.937 07	10.795 624	10.706 55	10.897 61	10.752 46	10.656 84	8.158 349 28	9.111 024 79
$\Delta n_{\max}$	0.0009	0.0011	0.0014	0.0016	0.0016	0.0012	0.0025	0.000 083
σ	0.0005	0.0006	0.000 67	0.000 84	0.0008	0.0005	0.0011	0.000 034
	a_0	$a_1\cdot 10^4\cdot\text{K}$	$a_2\cdot 10^6\cdot\text{K}^2$	a_0	$a_1\cdot 10^4\cdot\text{K}$	$a_2\cdot 10^6\cdot\text{K}^2$		
A	7.3377	5.534	−0.356	5.9613	7.178	−0.953	$A=a_0+a_1\cdot T+a_2\cdot T^2$	
	e_0	$e_1\cdot 10^4\cdot\text{K}$	$e_2\cdot 10^6\cdot\text{K}^2$	e_0	$e_1\cdot 10^4\cdot\text{K}$	$e_2\cdot 10^6\cdot\text{K}^2$		
$E_1^2/(\mu\text{m})^2$	3.791	−3.779	−1.121	4.7171	−3.237	−1.358	$E_1^2=e_0+e_1\cdot T+e_2\cdot T^2$	

$$n^2=A+\sum C_i/(E_i^2-E^2). \tag{7}$$

The constants, A, C_i, and E_i are determined empirically from the data. The constant, A, represents the contribution to the dielectric function of the highest energy transitions. For binary III–V compounds, we are considering three resonant energies, E_0, E_1, and E_2 and their associated values C_0, C_1, and C_2. Only the parameters with index 0 and 1 are additional fitting parameters. The direct band gap energy, E_Γ is close to E_0. The high-energy transitions in the visible to ultraviolet range will be considered by the coefficient, C_1, associated with the fitting energy, $E_1>E_0$. The extrapolation of all optical contribution to the high frequency dielectric constant, $\epsilon_0 n_\infty^2$ is given by

$$n_\infty^2=A+C_1/E_1^2+C_0/E_0^2. \tag{8}$$

With n_∞^2 and the relative static dielectric constant at $E=0$, ϵ_r, we can estimate the contribution of the lattice vibrations to the dielectric function. The contribution of the lattice vibration is approximated by a Lorentzian using the index 2

$$\epsilon_r=n_\infty^2+C_2/E_2^2=n_\infty^2\cdot(E_{\text{LO}}/E_{\text{TO}})^2, \tag{9}$$

where E_{LO} and E_{TO} stand for the longitudinal and transverse phonon energies, respectively. In the visible and near infrared regime this contribution is negative and amounts to a very small correction to the index of refraction. At $\lambda=3\ \mu$m, the longest wavelength used in our measurements, this correction is about $\Delta n=-0.002$ for GaAs, AlAs, and GaP. The five parameter fit is sensible to such a small correction. Accordingly, we retain this lattice contribution. The values for E_2 and C_2 are taken from the literature and are listed in Table II. The index of refraction is represented by

$$n^2=A+C_0/(E_0^2-E^2)+C_1/(E_1^2-E^2)+C_2/(E_2^2-E^2). \tag{10}$$

The parameters are determined from measured $n^2(\lambda)$ using a Gaussian approach to minimize the sum of the square residues. As the simple Sellmeier fits with only three independent parameters are quite good in a limited wavelength range, it will not be too surprising that the five parameter fits are not unique. This means that the fitting parameters can vary with E_0 and E_1 without strongly affecting the sum of the square residues. It appears that the observed variations depend on the residual errors of the measurements. The most precise data are on GaAs and GaP, where the variations are relatively small. We insist only that $A>1$, $C_0>0$, and $C_1>0$.

To determine the temperature dependence of the parameters, the following assumptions are made. (i) The fitting energy, E_0 is set equal to the direct band gap energy, E_Γ, whose temperature dependence is known. (ii) The energy E_1 and the parameter A are assumed to depend on temperature. (iii) The coefficients C_0 and C_1 do not depend on temperature. The independence of C_0 and C_1 on temperature can be grossly justified that they are proportional to the oscillator strength in a physical model. The new parameters $A(T)$ and $E_1(T)$ are determined similarly on the basis of the known $E_\Gamma(T)$. The best temperature dependence of the direct GaAs band gap seems to be given by Proctor[30]

$$E_{\Gamma\text{GaAs}}(T)=E_\Gamma(0)+S\cdot E_{\text{Deb}}[1-\coth(E_{\text{Deb}}/2k_BT)]+S_{\text{TO}}\cdot E_{\text{TO}}[1-\coth(E_{\text{TO}}/2k_BT)] \tag{11}$$

with the following values: $E_\Gamma(0)=1.5192$ eV, $E_{\text{Deb}}=15.9$ meV, $E_{\text{TO}}=33.6$ meV, $S=1.8$, and $S_{\text{TO}}=1.1$. The Boltzmann constant is $k_B=0.086\,1708$ meV/K. The representation of $E_\Gamma(T)$ depends on the phononic properties of the material. The energy, E_{Deb}, represents some average phonon energy related to the Debye temperature. For simplicity, we use the energy in terms of $(\mu\text{m})^{-1}$. The energies expressed in eV just have to be reduced by a factor of 1/1.239 856.

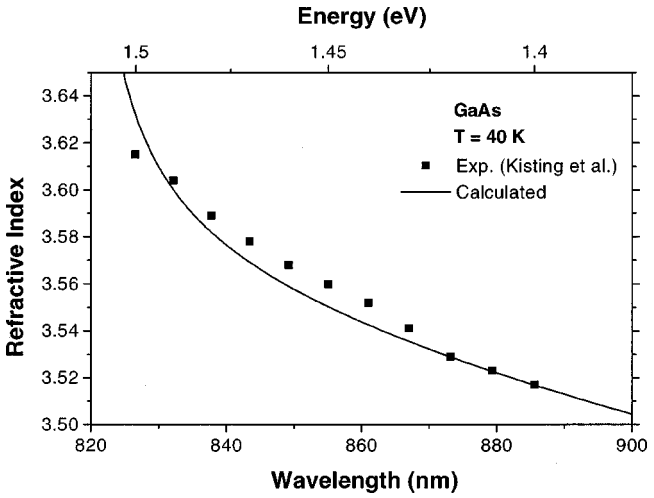

FIG. 3. Calculated and measured refractive index dispersion of GaAs at 40 K. The calculations are based on the new fitting procedure to Marple's data (see Ref. 9). The measured data are shown by the squares and are taken from Kisting *et al.* (see Ref. 16).

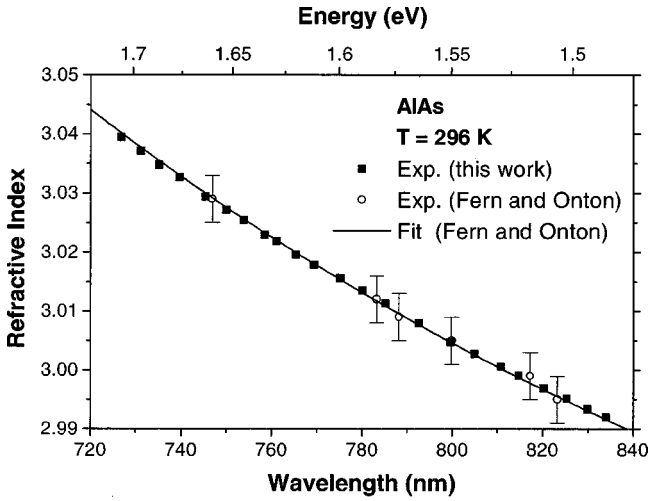

FIG. 4. Refractive index dispersion of AlAs. The solid squares give the data points determined with the grating coupling technique. The open circles show the data points from Fern and Onton (see Ref. 12). The experimental uncertainty of our data is approximately shown by the point size.

C. Results and discussion

Using the fitting procedures outlined above, we present the fitting parameters to the data for GaAs (Marple[9]), for AlAs (Fern and Onton[12] and this work), and for GaP (Nelson and Turner[28]) in Table II. To show the nonuniqueness of the fitting parameters, we present two fitting sets to the Marple data. No specific physical significance can be attributed to the values of E_1. The reason for retaining the second fit is explained in the next section. The maximum absolute deviation between the measured and fitted refractive index, $\Delta n_{\max}$ and the standard deviation, σ, are also listed to give a good characterization of the fits. The small correction due to the reststrahl band is taken into account.

1. GaAs

The Fit 1 is obtained for $E_0(T)=E_{\Gamma \mathrm{GaAs}}(T)$ by varying E_1 until a minimum of the sum of the square residues is achieved. As can be seen by the largest deviation in Table II, Fit 1 provides excellent fits to all data points at all temperatures. The fits are well within the precision of the data given in Marple's paper.[9] The values for n_∞^2 are slightly larger than that given by Marple.[9] We think that these extrapolated values are more precise than those found in the literature. The temperature dependence of A and E_1^2 have the forms $A=a_0+a_1\cdot T+a_2\cdot T^2$ and $E_1^2=e_0+e_1\cdot T+e_2\cdot T^2$, respectively. The fitted coefficients are given at the bottom of Table II. The coefficients of the temperature dependence of A and E_1 do not provide a vanishing temperature dependence at $T=0$. Only the direct band gap term has this character. The extrapolation of the fit parameters to 40 K is tested by comparing to the low temperature measurements by Kisting *et al.*[16] Figure 3 demonstrates the good agreement. It should be noted that the shortest wavelength is as close as 20 meV below the band gap energy. The predicted dispersion near the band gap is slightly stronger than that of the measurements. All of the data of Kisting *et al.*[16] agree quite well with the predictions of our simple model. Typical deviations from the measured data are $\Delta n \approx 0.005$. The maximum deviation from n is <0.014. Judging from the data scattering, we conclude that the measurements are considerably less precise than those of Marple.[9] Fit 2 deviates slightly more from the experimental data than Fit 1. But the deviations remain below 0.4% for all data points at all temperatures given by Kisting *et al.*[16] For this reason, we believe that the fits based on our simple assumptions represent the reality very well. For long wavelengths (5–20 μm), Cardona[31] gave a value for $(dn/dT)/n=4.5\times10^{-5}\,\mathrm{K}^{-1}$. Our calculation yields a value of $6.9\times10^{-5}\,\mathrm{K}^{-1}$. In view of the good agreement of the data close to the band gap, this discrepancy is rather surprising.

2. AlAs

The fitting of the data by Fern and Onton[12] is somewhat less precise than that of GaAs. One reason is certainly due to the reduced precision of the AlAs data at room temperature. The uncertainty of their refractive index measurements is given by them as 0.004. Unfortunately, no comprehensive study of the temperature dependence of the index of refraction exists.

Our data shown in Fig. 4 are limited to the grating coupling technique over a small spectral range, because AlAs strongly reacts with water and water vapor.[11] The thin GaAs protective layer permits us to use the grating coupling technique over a sufficiently long time interval. However, the extension of the spectral range with the transmission technique is very difficult. The surface oxidizes in air very rapidly after removing the layer from the substrate. It is very difficult to get a transmission spectrum with neatly resolved Fabry-Pérot oscillations. Although the free surface oxidizes immediately, we were able to observe Fabry-Pérot oscillations in transmission or reflection for a short time (approximately 5 min) after taking out the layer from the etchant. After several minutes, the surface degrades so heavily that the amplitudes of the oscillations decrease to zero. For this reason we use a miniature fiberoptic spectrometer[32] equipped

with a 2048 pixel CCD array to accelerate the data acquisition on the AlAs layers. The miniature spectrometer has a spectral resolution of 0.5 nm in the 0.7–1 μm range. The data thus obtained fit in precisely with those of Fern and Onton.[12] For the fitting, we use the combined data sets. Our fitting is simpler than that originally given by Fern and Onton.[12] The combined sets can also be well represented by a simple Sellmeier fit. However, the Sellmeier fit is not acceptable, if we later consider fits for the whole composition range of $Al_xGa_{1-x}As$. Lacking precise data on the temperature dependence of the direct band gap as well as the spread of the published direct gap data yields a large spread of the fitting parameters. The choice of the parameters is influenced by the entity of all measurements done on $Al_xGa_{1-x}As$, as is the Fit 2 of GaAs. Measurements of the direct band gap of $Al_xGa_{1-x}As$ indicate that the temperature dependence is close to that of GaAs. This is surprising, as the temperature dependence of the band gap is of a phononic nature quite dissimilar from GaAs. The chosen fit parameters are presented in Table II. As can be seen from Δn_{max} and σ, the fit parameters describe the data very well. As the bulk of the data is due to Fern and Onton,[12] we believe that they overestimated their errors.

3. GaP

As mentioned above, the case of GaP is quite interesting. First, the direct and, less importantly, the indirect band gaps are very close to the ones of AlAs. We take $E_{\Gamma GaP}$ of GaP as 2.85 eV. Second, the energy of the TO phonon, E_{TO}, is almost identical to that of AlAs. For our purposes, we take them as identical. Third, the very precise data set of Nelson and Turner[28] permits us to test the fitting procedures in a case where the relative and systematic errors cannot permit a very large uncertainty of the fitting parameters. Since the data are only available in the range $0.545\ \mu m < \lambda < .7\ \mu m$, this test is not as critical as one would like. For this reason, only the parameter set is presented, where $E_1 = E_{\Gamma GaP}$. The high precision of the data makes the correction of the reststrahl band meaningful in spite of its smallness. The values of σ and Δn_{max} attest to the high precision of the data. We think that the errors given by Nelson and Turner[28] are very conservative. Due to the small spectral range, a Sellmeier fit is possible, but it yields an increase of the standard deviation by a factor of 2.

IV. ANALYSIS OF $Al_xGa_{1-x}As$

The large numerical data set will not be presented in detail. The fitting procedure developed with the III–V binaries permit us to present the data in closed form. The deviations remain small, typically in the order of 0.1% over a large spectral range for $\lambda_\Gamma < \lambda < 3\ \mu m$. The wavelength, λ_Γ, corresponds to the direct energy gap. With the transmission method it is possible to measure the index of refraction in the indirect gap regime for Al concentrations, $x > 0.4$. Some samples have been measured at higher temperatures to provide the first data on the temperature dependence of $Al_xGa_{1-x}As$. Using the fitting procedure developed for the binary III–V compounds, we are also able to provide some analytical description of the temperature dependence of the index of refraction of $Al_xGa_{1-x}As$. It is important to note that the data reduction is strongly influenced by the precision of the measured Al concentration, x. An absolute uncertainty of x of only 0.5% implies a typical uncertainty of the refractive index of 0.3%. Near λ_Γ, this uncertainty can be even larger than 0.3%. The comparison of published data is quite difficult, because of systematic and random errors in the determination of the sample composition.[15] Valuable attempts to eliminate the uncertainty of the Al composition were made by Deri and Emanuel[6] to use the available data to derive a common sample concentration. We are not following this approach, because we present a comprehensive experimental study on the index of refraction below the band gap.

In our analysis, the primary concern is the internal consistency of the data. To achieve this goal within the measurement uncertainties, the fitting procedures developed above play an important role. Even if the fitting parameters have not a direct physical meaning other than $E_0 = E_\Gamma$, their qualitative character is of importance. The general fitting function of the refractive index has the modified form

$$n^2(x) = A(x) + C_0(x)/(E_0^2(x) - E^2) + C_1(x)/(E_1^2(x) - E^2) + R(x), \tag{12}$$

where x is the Al concentration. The reststrahl correction is given by $R(x)$. As the phonon structure of ternary materials cannot be described by an effective crystal approximation, we take the GaAs-like and the AlAs-like TO phonon energies as $E_2(x)$ and $E_3(x)$, respectively. The constants $C_2(x)$ and $C_3(x)$ are proportional to the oscillator strength of these phonons, respectively

$$R(x) = (1-x)\cdot C_2/(E_2^2(x) - E^2) + x\cdot C_3/(E_3^2(x) - E^2). \tag{13}$$

The reststrahl corrections are small in the binaries and in the ternaries. Together with the weak dependence of the GaAs- and the AlAs-like phonons on the Al concentration, we take for simplicity $E_2(x) = E_{2\ GaAs}$, $C_2 = C_{2\ GaAs}$, $E_3(x) = E_{2\ AlAs}$, and $C_3 = C_{2\ AlAs}$.

The compositional dependence of the fundamental band gap is based on the measurements by Bosio *et al.*[27]

$$E_\Gamma(x) = E_{\Gamma GaAs} + 1.36\cdot x + 0.22\cdot x^2. \tag{14}$$

Experiments by many authors show that the temperature dependence of $E_\Gamma(x)$ is practically identical to that of GaAs. This provides a possibility to also describe the temperature dependence of the refractive index of $Al_xGa_{1-x}As$. This will be discussed in the following subsections B and C.

A. Room temperature refractive index

A measurement result of the refractive index dispersion determined by the grating coupling technique under TE polarization at a temperature of 23.0 °C is shown in Fig. 5 for a sample with $x = 0.334$. The data obtained by the grating coupling method in the range $0.73\ \mu m < \lambda < 0.83\ \mu m$ can be well fitted with the three parameter Sellmeier equation. For the data shown in Fig. 5 by the squares, the Sellmeier parameters are: $A = 7.0435$, $C_1 = 14.1179\ (\mu m)^{-2}$, and E_1^2

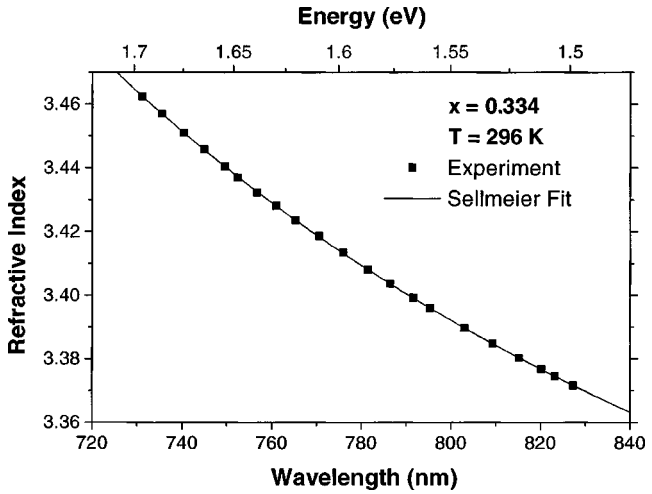

FIG. 5. Refractive index dispersion of sample with $x=0.334$ determined with the grating coupling technique at $T=23\,^{\circ}\mathrm{C}$. The data are fitted with a three parameter Sellmeier fit.

$=4.7257\,(\mu\mathrm{m})^{-2}$. The fit yields $\sigma=1.4\times10^{-4}$ and $\Delta n_{\max}=3.1\times10^{-4}$. This good fit attests to the high relative precision of the data. But the precision of the experimental data and/or the fitting interval are not high enough to arrive at unique parameters with a fit that contains four free parameters according to Eqs. (12)–(14).

For wavelengths outside the tuning range of the laser, the refractive index is measured by the transmission method for $\lambda<3$ μm. The short wavelength limit depends on the Al concentration and is $\lambda>0.47$ μm for $x=0.865$. With the precise knowledge of the refractive index between 0.73 and 0.83 μm, we unambiguously determine the interference order number and the layer thickness. The thickness of the layers with etched-off substrates is typically 2%–4% lower than that of Table I determined by the grating coupling technique. This systematic difference is caused by a slight etching of the $Al_xGa_{1-x}As$ layer due to the finite selectivity of the etching solutions.[22,23] The refractive index at the wavelengths of the transmission maxima and minima is then calculated according to Eq. (3). The absolute precision of the index values is mainly limited by the wavelength accuracy of the spectrometer. It is estimated to be $\Delta n<0.004$ for 0.5 μm$<\lambda<2$ μm and $\Delta n<0.008$ for 2 μm$<\lambda$.

A choice of four free fitting parameters is given in Table III. The fitting curve according to Eq. (12) with the parameters of Table III cannot be distinguished from the three parameter Sellmeier fit of Fig. 5. All samples with $0.17<x\leqslant1$ can be similarly fitted in the interval 0.73 μm$<\lambda<0.83$ μm with standard deviations $<10^{-3}$. Outside of this wavelength range, simple Sellmeier fits are no longer accurate and the parameters of Table III have to be used.

Table III gives the best fitting parameters (Fit 1) to the combined refractive index dispersion data. The parameters are obtained from each sample by a least square approach using $E_0=E_\Gamma$ according to Eqs. (12–14). In spite of the smallness of the reststrahl band contribution, the parameters are affected by it in a systematic fashion. The standard deviation, σ, is for all Al concentrations <0.0011. The largest absolute deviation from the measured refractive index, $\Delta n_{\max}$, is <0.0031. This is well within the expected measurement uncertainties. The parameters of Table III thus represent the entity of our data set very well.

We note the following general trends. Parameter, A, decreases with increasing Al concentration, x, while C_1 and E_1 increase with x. A similar trend but with stronger fluctuations is seen for C_0. We also remark that the fit to GaP yields the largest C_0 value of the binaries. The contribution of the direct gap to the dielectric function is seen to be small in all cases for energies sufficiently below the direct band gap. For practical purposes, we have an excellent agreement between measurement and fit for an energy difference of 30 meV that corresponds to $0.024\,(\mu\mathrm{m})^{-1}$ for direct band gap materials at room temperature. At low temperatures, the tolerable energy difference is reduced to about 20 meV) as demonstrated in Fig. 3. The indirect band gap material with $x=0.865$ shows good agreement for all data points, where the energy difference at the highest photon energy measured is 0.186 eV or $0.15\,(\mu\mathrm{m})^{-1}$ below its direct band gap. The indirect gap of ~2.1 eV is considerably lower than our highest measured energy of 2.6 eV. The absolute deviation of $\Delta n_{\max}=0.0029$ is in the infrared regime, where our measurement accuracy is reduced. The measured refractive index data are given in Fig. 6. The fitting curves to the data are described below.

The relative optical dielectric constants, n_∞^2, are also listed in Table III, and they are plotted in Fig. 7. At T

TABLE III. Parameters to determine $n^2(x,\lambda)$ of $Al_xGa_{1-x}As$ at 23 °C. All fits are made by setting E_0 to the direct band gap of the respective material composition. The relative high frequency dielectric constants, n_∞^2, the standard deviation, σ, and the largest absolute deviation, $\Delta n_{\max}$, are also given. At $x=0.334$, the data are limited to the wavelength range 0.73 μm$<\lambda<0.83$ μm.

x	A	$C_1/(\mu\mathrm{m})^2$	$E_1^2/(\mu\mathrm{m})^2$	$C_0/(\mu\mathrm{m})^2$	$E_0^2/(\mu\mathrm{m})^2$	n_∞^2	$10^3\cdot\sigma$	$10^3\cdot\Delta n_{\max}$
0	7.4704	12.361 51	3.581	0.0154	1.323	10.93	0.5	0.9
0.176	3.1739	53.3589	7.486	0.0622	1.855	10.34	1.1	2.5
0.334	3.3646	50.372 98	7.835	0.0912	2.383	9.83	0.2	0.3
0.410	4.5043	36.7799	7.151	0.0677	2.626	9.67	1.1	3.1
0.427	4.2524	38.5382	7.227	0.0552	2.607	9.61	1.0	2.9
0.615	2.9993	59.0641	9.791	0.2833	3.600	9.11	1.0	2.4
0.753	2.5234	67.5218	10.975	0.3460	4.206	8.76	0.9	2.5
0.865	1.6989	82.5887	12.401	0.3759	5.066	8.43	1.0	2.9
1	2.2863	72.927 14	12.507	0.3315	5.878	8.17	0.9	2.3

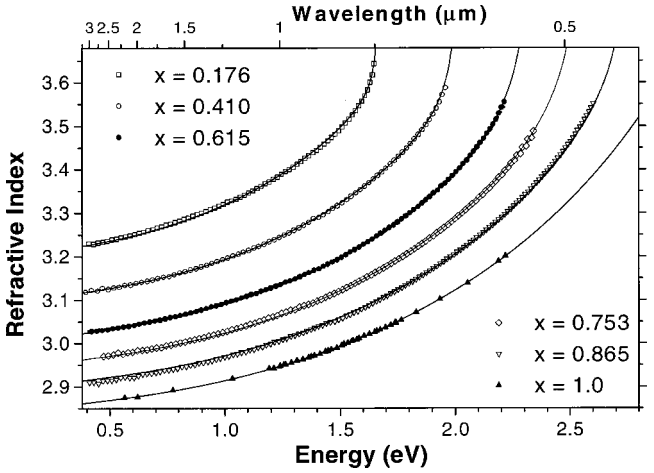

FIG. 6. Refractive index dispersion obtained by combining the results of the grating coupling technique and transmission spectroscopy at $T=23\,^{\circ}\mathrm{C}$. The Al concentration is indicated by the inset. The solid lines represent the fits using the parameters of Table IV.

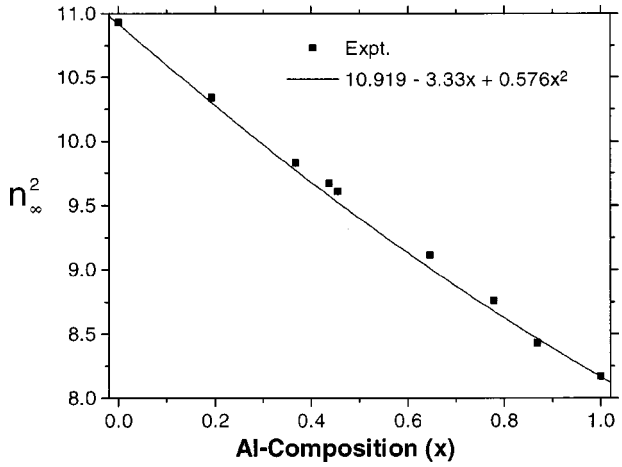

FIG. 7. Relative high frequency dielectric constant, n_∞^2, as a function of Al concentration at $T=23\,^{\circ}\mathrm{C}$.

$=23\,^{\circ}\mathrm{C}$, the slight bowing of the data can be described by the following fitting relation:

$$n_\infty^2 = 10.919 - 3.330\cdot x + 0.576\cdot x^2. \tag{15}$$

The standard deviation is 0.028. The uncertainty of n_∞^2 is difficult to estimate, as n_∞^2 weakly depends on the fitting procedure. This is illustrated in Table II for the case of GaAs, where Fit 1 and Fit 2 yield values of 10.937 and 10.898, respectively at 28 °C. The values derived from Eq. (15) are consistent with those found in the literature.[12,33]

As the fitting parameters of our qualitative physical model represent some well-established trends, it is worthwhile to attempt a pragmatic physical interpretation. This should permit us to establish some practical analytical representation of the entire data sets.

B. Analytical representation of the *x* dependence of the refractive index

To obtain an analytical description of the $Al_xGa_{1-x}As$ refractive index as a function of x, we fit polynomials to the compositional dependence of the fitting parameters. However, a direct polynomial fit as a function of the Al-concentration is not feasible with the parameters given in Table III. Systematic and random errors are the most likely cause for some of the uncertainty of the fit parameters. This is quite evident if one looks at the behavior of C_0 over the whole concentration range. Similarly, the fitting parameter A rapidly decreases at low Al concentrations. For physical reasons, we expect a smooth dependence of the parameter on the Al concentration. This can be forced by considering fits with parameters that degrade the agreement somewhat. This is the precise reason, why we have considered fit 2 for GaAs and accepted a fit for C_0 with a maximum at $x=0.75$. The temperature dependence of the index of refraction is well described for GaAs for either fit parameter set. Because the direct band gap of $Al_xGa_{1-x}As$ follows the temperature dependence of GaAs, it is proposed that the refractive index only depends on the same temperature parameters for A, E_1, and E_0 of GaAs. We define $A_0=A_{\mathrm{GaAs}}$ and $E_{10}=E_{1\mathrm{GaAs}}$. The result of this proposition to model the temperature dependence will be examined below. With these considerations, we achieve a useful fit to all data with the parameters given in Table IV. The fit parameters have the following form:

TABLE IV. Parameters to calculate $n^2(x,\lambda,T)$. The temperature dependence is given by the temperature dependent parameters of GaAs designated by $A_0(T)$, $E_{10}^2(T)$ and $E_{\Gamma\mathrm{GaAs}}(T)$. The parameters have the form $c(x,T)=c_0(T)+c_1\cdot x+c_2\cdot x^2+c_3\cdot x^3+c_4\cdot x^4+c_5\cdot x^5$. The quality of the fit for the measured data at $T=23\,^{\circ}\mathrm{C}$ is also indicated by σ and $\Delta n_{\max}$.

						QUALITY OF FIT		
$c(x,T)$	A	$C_1/(\mu\mathrm{m})^2$	$E_1^2/(\mu\mathrm{m})^2$	$1/C_0/(\mu\mathrm{m})^2$	$E_0/(\mu\mathrm{m})$	x	$10^3\cdot\sigma$	$10^3\cdot\Delta n_{\max}$
						0	0.8	1.6
						0.176	2.5	4.4
c_0	$A_0(T)$	21.5647	$E_{10}^2(T)\cdot(\mu\mathrm{m})^2$	50.535	$E_{\Gamma\mathrm{GaAs}}(T)\cdot(\mu\mathrm{m})$	0.334	0.6	0.9
c_1	−16.159	113.74	11.006	−150.7	1.1308	0.410	2.5	9.5
c_2	43.511	−122.5	−3.08	−62.209	0.1436	0.427	9.9	47
c_3	−71.317	108.401	0	797.16	0	0.615	1.9	6.1
c_4	57.535	−47.318	0	−1125	0	0.753	1.4	3.6
c_5	−17.451	0	0	503.79	0	0.865	3.1	8.1
						1	0.9	2.5

$$c(x,T)=c_0(T)+c_1\cdot x+c_2\cdot x^2+c_3\cdot x^3+c_4\cdot x^4+c_5\cdot x^5. \tag{16}$$

The parameter, $c(x,T)$ stands for A, $1/C_0$, E_0, C_1, and E_1^2. The constants, c_i, with $i=0$, 1, 0.5 are the factors of the corresponding power of the Al-concentration, x^i. The temperature dependence given by $c_0(T)$ is thus rigidly following that of GaAs. The parameters of Table IV fit the data well as shown in Fig. 6.

The data of $x=0.427$ (not shown in Fig. 6) deviates in the band gap region. It is highly probable that the poor fit in this case is caused by some systematic error. Four facts are worth noting: (i) The proximity to the sample with $x=0.41$ should yield fitting parameters that are very close. But inspection of Table III reveals significantly different values for C_0. (ii) Good fitting can be forced for either one of these two concentrations but not together. (iii) Poor fitting was also obtained for one of these concentrations, if a radically different fitting method is used such as given by Deri and Emanuel.[6] (iv) The sample with $x=0.427$ is the only one made by MBE. Effects due to stoichiometry or homogeneity cannot be excluded. Because excellent fits to both compositions are obtained by individual fitting, we cannot resolve this discrepancy. The overall analytical fits have systematic deviations generally much smaller than 0.3%.

The origins of the possible systematic errors are sample homogeneity and corrections in the transmission measurements due to the thin, protective GaAs layer. The near field mode shapes shown in Fig. 2 are very sensitive to any striations caused by systematic index fluctuations. As we have not detected any significant deformation of the modal near fields, we consider Al concentration fluctuations as a highly unlikely cause of systematic errors. The corrections due to the protective layers are also very small. However, they strictly depend on the dispersion of the GaAs that we have not taken into account. The effective thickness in Eq. (3) should be corrected for dispersion of the GaAs refractive index outside of the wavelength range from 0.73 μm$<\lambda<$0.83. We justify this neglect by the fact that the errors of the spectrometers are larger than these dispersion corrections.

It should be noted that the optical dielectric constants derived from the analytical x dependence deviate only slightly from the values obtained from Table III. The deviations remain well within the experimental uncertainties, but the bowing parameters are strongly affected.

C. Temperature coefficient

All refractive index data presented thus far are obtained at a temperature of 23.0 °C. The high accuracy of the grating coupling technique also permits us to measure the temperature dependence of the refractive index. To this end, the TE mode indices are determined at various temperatures from 15 to 40 °C and fitted linearly to obtain the temperature coefficient dn/dT at room temperature. The typical standard deviation of the fits is $\sim 2\times 10^{-5}\,\mathrm{K}^{-1}$.

The grating period is determined at each measurement temperature, to account for the linear expansion of the grating with temperature. We obtain a mean value of the linear expansion coefficient, $(d\Lambda/dT)/\Lambda=10^{-6}\,\mathrm{K}^{-1}$. This value is consistent with the thermal expansion coefficient of GaAs at room temperature.[34]

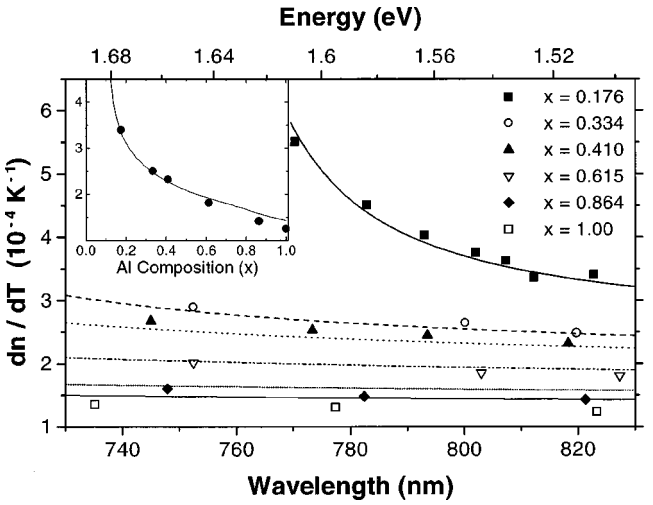

FIG. 8. Wavelength dependence of the temperature coefficient of the refractive index, dn/dT. The connecting lines are calculated from the model parameters given in Table II and Table IV.

Figure 8 shows the results for wavelengths between 740 and 820 nm. The sample with $x=0.176$ is measured close to the band gap. A strong wavelength dependence of the temperature coefficient is observed in this sample.[35] The other samples show only a slight linear decrease with increasing wavelength. The measurement range for the AlAs sample is far from the band gap and dn/dT is practically independent of λ at a value of approximately $1.25\times 10^{-4}\,\mathrm{K}^{-1}$. This value is in agreement with the long-wave limit of dn/dT as determined in Refs. 36 and 37.

There are no data on the temperature coefficient of $Al_xGa_{1-x}As$ in the literature. Our measurements fill this lack of information and permit us to test our simple model given above. The inset of Fig. 8 shows the temperature dependence on the Al concentration for a fixed $\lambda=0.82$ μm. The agreement is quite remarkable. Accordingly, our simple model gives a comprehensive description of the refractive index of $Al_xGa_{1-x}As$ as a function of wavelength, composition, and temperature.

D. Piezobirefringence

In the Appendix, we show by Eqs. (19) and (20) that the difference in effective index between TE and TM polarization is negligibly small for thick and homogeneous waveguide layers. Therefore, any index difference depending on the polarization direction is caused by the birefringence of the guiding layer material. Figure 2 shows a noticeable difference in the angular resonance positions of TE and TM modes. This birefringence can be attributed to internal strain.[38]

The strain components parallel and perpendicular to the layer plane are determined by HRXRD measurements by employing symmetrical (004), (006) and asymmetrical reflections (444), (115). The biaxial stress, σ_b, is calculated[39]

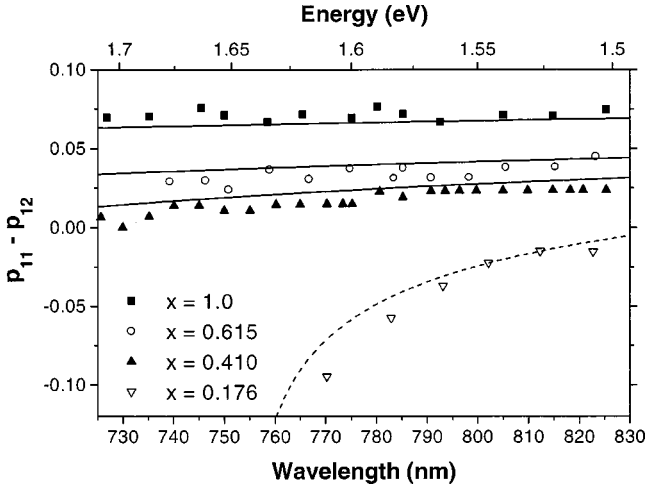

FIG. 9. Dispersion of the elasto-optic coefficient $p_{11}-p_{12}$ obtained by grating coupling measurements for different polarization directions at $T=23\,^{\circ}\mathrm{C}$. The sample composition is given by the inset. The lines are fits using the empirical model using the parameters.

from the strain and the elastic constants, C_{11} and C_{12}, determined directly by near infrared Brillouin scattering on the same samples.[26] The effective refractive indices, n_{TM} and n_{TE}, for TE and TM polarization, respectively, are measured by the grating coupling technique. The elasto-optic component $p_{11}-p_{12}$ is calculated according to the following relation:[40]

$$p_{11}-p_{12}=[(n_{\mathrm{TM}}^2-n_{\mathrm{TE}}^2)/n_0^4]\cdot(C_{11}-C_{12})/\sigma_b, \tag{17}$$

where n_0 is the refractive index of the unstrained crystal.

Figure 9 gives the measured dispersion of the elasto-optic coefficient $p_{11}-p_{12}$ for samples with the following Al compositions: 0.176, 0.41, 0.615, and 1. The absolute uncertainty is approximately 0.015. The rather large measurement uncertainty can be ascribed to the limited precision of our goniometer. Our results on the birefringence of sample with $x=0.41$ reasonably agree with the measurements of van der Ziel and Gossard[13] on a 4.6-μm-thick $Al_{0.48}Ga_{0.52}As$ layer. At 0.8 μm, we get a birefringence of $\Delta B=n_{\mathrm{TE}}-n_{\mathrm{TM}}=5\times10^{-4}$, and the calculated interpolation curve of Ref. 13 gives a value of $\Delta B=5.8\times10^{-4}$.

To get an analytic expression of the data, we use the oscillator model describing the spectral dependence of the elasto-optic coefficients of III–V semiconductors presented by Adachi and Oe.[41] This model uses two fitting parameters (called ''*C*'' and ''*D*'' in Ref. 41) which have to be adapted to describe experimental values of elasto-optic coefficients. Different sets for the compositional dependence of these parameters have been proposed for $Al_xGa_{1-x}As$ (Refs. 41 and 42), but both did not reproduce our experimental values very well. This is not surprising, since the compositional dependence of the fitting parameters was obtained by linear interpolation of the values of only two experimental data sets (for GaAs[43] and $Al_{0.5}Ga_{0.5}As$[13]).

To improve the consistency between the model and our experimental data, we adapted the fitting parameters (C^* and D^*), so that they give a better description of our measurements. We obtain the following compositional relationship for the model parameters:

$$C^*(x)=-0.46+0.32x,$$
$$D^*(x)=2.22-1.52x+0.59x^2. \tag{18}$$

The lines in Fig. 9 represent the calculated dispersion of $p_{11}-p_{12}$ using the above fitting parameters. Since our measurements cover a limited spectral window, we do not expect that our proposed values for the compositional dependence of the model parameters are applicable over the full energy range. But at least in the near infrared, they provide a much better description of the absolute value of $p_{11}-p_{12}$ than the original values proposed by Adachi.[41,42] To get a reliable modeling of the elasto-optic dispersion, measurements with a more accurate angular reading and over a larger spectral range would be necessary.

V. SUMMARY

We have presented an extensive investigation on the refractive index of $Al_xGa_{1-x}As$ epitaxial layers. A combination of a grating coupling technique and transmission spectroscopy is used to precisely determine the room temperature refractive index from the direct band gap up to $\lambda<3$ μm. In the wavelength range from 0.73 μm to 0.83 μm, the dispersion of the refractive index is determined by the grating coupling technique with an estimated uncertainty of $\Delta n<5\times10^{-4}$. Our values for AlAs are within the experimental accuracy in perfect agreement with literature data.[12] However, our values are an order of magnitude more accurate than the published data in this restricted wavelength interval.

The $Al_xGa_{1-x}As$ data are compared with an analytical expression from modeling the index below the band gap. This comparison shows that the determination of composition is the most critical issue. Bearing in mind that most compositional analysis techniques have uncertainties of 1.0% or larger, some discrepancies with literature data are expected.

The high accuracy of the grating coupling measurements also permits us to analyze the spectral dependence of the temperature coefficient of the refractive index. The simple model using the temperature dependence of the index of refraction of GaAs as a basis agrees remarkably well for all Al concentrations.

The Fabry-Pérot oscillations observed in transmission and reflection from layers with etched-off substrates are analyzed. They permit us to obtain the refractive index data from the direct band gap up to wavelengths of 3 μm. The high frequency dielectric constants show a weak quadratic dependence on the Al concentration. They are affected by the correction due to the reststrahl bands by up to 1%. With our fitting procedure tested on binary compounds, we arrive to describe quite accurately the compositional dependence of the dispersion and the temperature dependence of the index of refraction. The satisfactory fit to all data attests to the high consistency of the determined Al concentration.

We demonstrate that the grating coupling technique is sufficiently precise to determine the strain birefringence introduced by the residual mismatch of the lattice constants between the epitaxial layers and the substrate. The magnitude of the strain is determined by HRXRD. The elasto-optic coefficient, $p_{11}-p_{12}$, can then be determined. A comparison with a semiempirical model by Adachi and Oe[41,42] shows that their parameters do not provide a satisfactory description of our experimental values. For this reason, we give a new set of fitting parameters that yield an improved agreement with the experimental results.

It is also important to mention that to second order in d there is no significant difference in the effective index for TE and TM modes, and the third order corrections are smaller than 2×10^{-5} for our structures. The waveguide theory only yields a negligible structural birefringence due to the TE and TM modes. Therefore, any experimentally observed difference in the effective index of TE and TM modes has to be attributed to an intrinsic birefringence of the guiding layer material.

APPENDIX: LEAKY MODES IN IMPROPER WAVEGUIDES

Following the treatment of Hall and Yeh[44] it can be shown that the propagation constants of leaky modes in a simplified three layer improper waveguide structure are expressed by the following relations:

$$\beta_{\mathrm{TE}}=n_2k_0\left[1-\frac{1}{2}\left(\frac{m\pi}{n_2k_0d}\right)^2\right]-i\left(\frac{m\pi}{k_0d}\right)^2\times\left[\frac{1}{dn_2\sqrt{n_1^2-n_2^2}}+\frac{1}{dn_2\sqrt{n_3^2-n_2^2}}\right], \tag{19}$$

$$\beta_{\mathrm{TM}}=n_2k_0\left[1-\frac{1}{2}\left(\frac{m\pi}{n_2k_0d}\right)^2\right]-i\left(\frac{m\pi}{k_0d}\right)^2\times\left[\frac{(n_1/n_2)^2}{dn_2\sqrt{n_1^2-n_2^2}}+\frac{(n_3/n_2)^2}{dn_2\sqrt{n_3^2-n_2^2}}\right]. \tag{20}$$

The propagation constants for TE and TM polarization are β_{TE} and β_{TM}, respectively. The wave number of the light in vacuum is k_0, and n_2 is the refractive index of the core material with thickness d. The refractive indices of the cladding layers are n_1 and n_3, respectively.

Equations (19) and (20) show that the cladding layers with n_1, $n_3>n_2$ give only a contribution to the attenuation coefficient (imaginary part of β). In the case of an asymmetrical improper waveguide with $n_1>n_2>n_3$, only the substrate with n_1 gives a loss contribution, while the top layer with n_3 provides a small correction to the phase constant (real part of β). Since the top layer of our structures is mainly composed of photoresist and air, this condition is fulfilled. For this case, the contribution to the effective index of a 4-μm-thick guiding layer is $\Delta n<2\times10^{-4}$ for our wavelength range. The absorbing substrate gives a small contribution to the phase constant via the imaginary part of the substrate refractive index, but this part is even much smaller and amounts to $\Delta n=3\times10^{-5}$ in the worst case.

Since the estimated contributions of the cladding layers are smaller than the absolute precision of our measurements, we neglect them in the evaluation. We can determine the refractive index, n, of the improper waveguide core simply by measuring the real part of the propagation constant, without taking the exact structure and refractive indices of the cladding layers into account.

[1] F. Stern, Phys. Rev. **133**, 1653 (1964).
[2] M. A. Afromowitz, Solid State Commun. **15**, 59 (1974).
[3] S. Adachi, Phys. Rev. B **38**, 12345 (1988).
[4] D. W. Jenkins, J. Appl. Phys. **68**, 1848 (1990).
[5] C.-H. Lin and J. M. Meese, J. Appl. Phys. **74**, 6341 (1993).
[6] R. J. Deri and M. A. Emanuel, J. Appl. Phys. **77**, 4667 (1995).
[7] Y. Kokubo and I. Ohta, J. Appl. Phys. **81**, 2042 (1997).
[8] J. Zheng, C.-H. Lin, and C. H. Kuo, J. Appl. Phys. **82**, 792 (1997).
[9] D. T. F. Marple, J. Appl. Phys. **35**, 1241 (1964).
[10] H. C. Casey, Jr., D. D. Sell, and M. B. Panish, Appl. Phys. Lett. **24**, 63 (1974).
[11] D. E. Aspnes, S. M. Kelso, R. A. Logan, and R. Bhat, J. Appl. Phys. **60**, 754 (1986).
[12] R. E. Fern and A. Onton, J. Appl. Phys. **42**, 3499 (1971).
[13] J. P. van der Ziel and A. C. Gossard, J. Appl. Phys. **48**, 3018 (1977).
[14] G. J. Sonek, J. M. Ballantyne, Y. J. Chen, G. M. Carter, S. W. Brown, E. S. Koteles, and J. P. Salerno, IEEE J. Quantum Electron. **QE-22**, 1015 (1986).
[15] R. G. Kaufmann, G. R. Hulse, D. J. Vezzetti, A. L. Moretti, K. A. Stair, G. P. Devane, and T. E. Bird, J. Appl. Phys. **75**, 8053 (1994).
[16] S. R. Kisting, P. W. Bohn, E. Andideh, I. Adesida, B. T. Cunningham, G. E. Stillman, and T. D. Harris, Appl. Phys. Lett. **57**, 1328 (1990).
[17] F. Vasey, J. M. Stauffer, Y. Oppliger, and F. K. Reinhart, Appl. Opt. **30**, 3897 (1991).
[18] P. M. Martin, E. M. Skuori, L. Chusseau, and C. Alibert, Appl. Phys. Lett. **67**, 881 (1995).
[19] L. Chusseau, P. Martin, C. Brasseur, C. Alibert, P. Hervé, P. Arguel, and F. Lozes-Dupuy, Appl. Phys. Lett. **69**, 3054 (1996).
[20] U. Marti, M. Proctor, D. Martin, F. Morier-Genoud, B. Senior, and F. K. Reinhart, Microelectron. Eng. **13**, 391 (1991).
[21] C. Gourgon, F. Filipowitz, J. Robaday, D. Martin, Y. Magnenat, P. C. Silva, F. Bobard, and F. K. Reinhart, presented at the 6th International Symposium on Nanostructures: Physics and Technology, St. Petersburg, Russia, June 22–26, 1998, unpublished.
[22] R. A. Logan and F. K. Reinhart, J. Appl. Phys. **44**, 4172 (1973).
[23] G. C. DeSalvo, W. F. Tseng, and J. Comas, J. Electrochem. Soc. **139**, 831 (1992).
[24] C. Bassignana, D. A. Macquistain, R. W. Streater, G. C. Hillier, R. Packwood, and V. Moore, J. Cryst. Growth **172**, 25 (1997).
[25] S. Gehrsitz, H. Sigg, N. Herres, and F. K. Reinhart, *Proceedings of the 24th International Conference on the Physics of Semiconductors*, Jerusalem, Aug. 2–7, 1998, edited by D. Gershoni (World Scientific, Singapore, 1999), Compact Disk.
[26] S. Gehrsitz, H. Sigg, N. Herres, K. Köhler, K. Bachem, and F. K. Reinhart, Phys. Rev. B **60**, 11601 (1999).
[27] C. Bosio, J. L. Staehli, M. Guzzi, G. Burri, and R. A. Logan, Phys. Rev. B **38**, 3263 (1988).
[28] D. F. Nelson and E. H. Turner, J. Appl. Phys. **39**, 3337 (1968).
[29] C. Tanguy, J. Appl. Phys. **80**, 4626 (1996).
[30] M. Proctor, thesis No. 1133, Swiss Federal Institute of Technology, Lausanne, Switzerland (1993).
[31] M. Cardona, *Proceedings International Conference, Semiconductor Physics*, Prague, 1960 (Czech. Acad. Sci., Prague, and Academic, New York, 1961), p. 388.
[32] Dual fiberoptic spectrometer from Ocean Optics, Inc., model SD2000, equipped with a 600 lines/mm blazed grating and a 2048 pixel CCD array.
[33] J. S. Blakemore, J. Appl. Phys. **53**, R123 (1982).
[34] S. Adachi, in *Properties of Gallium Arsenide*, 3nd ed., edited by M. R. Brozel and G. E. Stillman (Inspec IEE, London, 1996), Chap. 1.6, p. 23.

[35] M. Bertolotti, V. Bogdanov, A. Ferrari, A. Jascow, N. Nazorova, A. Pikhtin, and L. Schirone, J. Opt. Soc. Am. B **7**, 918 (1990).
[36] J. Talghader and J. S. Smith, Appl. Phys. Lett. **66**, 335 (1995).
[37] H. G. Grimmeis and B. Monemar, Phys. Status Solidi A **5**, 109 (1971).
[38] F. K. Reinhart and R. A. Logan, J. Appl. Phys. **44**, 3171 (1973).
[39] J. F. Nye, *Physical Properties of Crystals* (Clarendon, Oxford, 1989).
[40] J. E. Raynolds, Z. H. Levine, and J. W. Wilkins, Phys. Rev. B **51**, 10477 (1995).
[41] S. Adachi and K. Oe, J. Appl. Phys. **54**, 6620 (1983).
[42] S. Adachi, J. Appl. Phys. **58**, R1 (1985).
[43] C. W. Higginbotham, M. Cardona, and F. H. Pollak, Phys. Rev. **184**, 821 (1969).
[44] D. B. Hall and C. Yeh, J. Appl. Phys. **44**, 2271 (1973).